Effects of the air ducts layout in the back wall on the heat transfer and storage characteristics of active heat storage back wall of solar greenhouse

Yachen Sun[1,5†], Cuinan Wu[2†], Chenmeng Zhu[3], Guoliang Li[4], Yanfei Cao[5], Zhirong Zou[5], Encai Bao[2*]

(1. *College of Architecture and Urban Planning, Tongji University, Shanghai 200092, China*;
2. *Institute of Agricultural Facilities and Equipment, Jiangsu Academy of Agricultural Science, Key Laboratory of Protected Agriculture Engineering in the Middle and Lower Reaches of Yangtze River, Ministry of Agriculture and Rural Affairs, Nanjing 210014, China*;
3. *Fudan Univeristy, Shanghai 200433, China*;
4. *College of Civil Engineering, Tongji University, Shanghai 200092, China*;
5. *Key Laboratory of Protected Horticultural Engineering in Northwest, Ministry of Agriculture and Rural Affairs, Department of Horticulture, Northwest A & F University, Yangling 712100, Shaanxi, China*)

Abstract: Solar greenhouses have been widely developed in China. Active heat storage walls using air ducts arranged in the walls can improve the walls' thermal performance and indoor temperatures of solar greenhouses. In the present work, three kinds of air duct layouts, namely straight-up-and-down duct (Z), fork-shaped top-in- bottom-out distribution duct (DF), and "±"-shaped top-in-side-out distribution duct (CF) are designed. The effect of the three air duct layouts on the heat transfer and storage characteristics of the back wall is studied using the computational fluid dynamics (CFD) method. Results show that after the same time period, the transferred heat amount in the back wall with duct DF is the largest, while that with duct CF is slightly greater than that with duct Z. The temperature of the back walls with air ducts is higher than that without air ducts. The air duct DF is the optimal among the three kinds of air duct layouts. The greenhouse with the duct DF in the back wall shows the most obviously increased indoor average temperature, the highest temperature at night, and the most uniform temperature.

Keywords: active heat storage, heat transfer, air duct layout, solar greenhouse, CFD
DOI: 10.25165/j.ijabe.20251804.7785

Citation: Sun Y C, Wu C N, Zhu C M, Li G L, Cao Y F, Zou Z R, et al. Effects of the air ducts layout in the back wall on the heat transfer and storage characteristics of active heat storage back wall of solar greenhouse. Int J Agric & Biol Eng, 2025; 18(4): 63–70.

1 Introduction

Solar greenhouses have been widely developed in China and play a dominant role in winter vegetable supply for Northern China[1]. Besides load bearing and heat preservation, the storage and release capacity of solar greenhouse walls play a vital role in maintaining winter production[2]. Many efforts, including adopting new materials and optimizing wall structure, have been put forth to improve the heat storage and insulation capacity of the wall[3-7]. Among them, the active storage wall by means of air convection in the wall has attracted particular attention due to the fact that it can improve the air flow in the greenhouse and also the heat storage and release performance of the wall, besides being cost-effective and easy to implement[8-10]. For example, compared with the traditional wall, the hollow wall can effectively enhance indoor temperature at night and inhibit high temperature at noon due to air convection and heat storage. It is reported that the heat storage of the hollow wall during daytime is increased by 15.1%, the heat release at night is increased by 14.7%, and the minimum temperature at night of the greenhouse is increased by 2.2ºC, respectively[9]. However, it can be imagined that the natural air convection is inefficient, while forced convection by a fan can improve heat transfer. Moreover, the hollow part will seriously weaken the bearing capacity of the wall, especially for loess walls, which leads to a potential risk of collapse.

Research and applications have revealed that using an air circulator with forced convection can improve the indoor temperature and the uniformity of temperature in greenhouse[11]. It has also been confirmed that using forced convection by a fan in air ducts arranged in the back wall can significantly increase heat storage in the wall from the high-temperature indoor air, and increases indoor temperature at night in return[12]. However, the limited and uneven heat storage range in the wall using a one-way duct is a concern. It has been revealed that different airflow directions, i.e., top-in-top-out, side-in-top-out, and side-in-side-out, in air ducts arranged in the back wall have a significant effect on the heat transfer characteristics of the active heat storage back wall of the solar greenhouse[13]. Assuming the inlet temperature is the same, it has been demonstrated that the outlet temperature of the top-in-top-out air duct is the lowest, while that of the side-in-top-out is the highest[13]. The above results indicate that the amount and the range of transferred heat of the top-in-top-out air duct is the highest, while that of the side-in-top-out is the lowest. However, it should be noted

Received date: 2023-07-11 **Accepted date:** 2024-10-18
Biographies: Yachen Sun, PhD, research interest: facility horticulture, Email: sunyachen1993@163.com; **Cuinan Wu**, PhD, Assistant Research Fellow, research interest: facility horticulture engineering, Email: wucuinan@126.com; **Chenmeng Zhu**, MBA, research interest: organizational management, Email: zhuchenmeng@fudan.edu.cn; **Guoliang Li**, MS, research interest: intelligent construction, Email: 1250869lgliang@tongji.edu.cn; **Yanfei Cao**, PhD, research interest: greenhouse structure optimization, Email: caoyanfei@nwsuaf.edu.cn; **Zhirong Zou**, PhD, Professor, research interest: facility horticulture, Email: zouzhirong2005@163.com.
†These authors contribute equally to this research.
***Corresponding author: Encai Bao**, PhD, Assistant Research Fellow, research interest: facility horticulture engineering. Institute of Agricultural Facilities and Equipment, Jiangsu Academy of Agricultural Science, Nanjing 210014, China. Tel: +86-17768103527, Email: baoencai1990@163.com.

that the length of the top-in-top-out air duct is longer than the others due to the fact that it is along a circuitous path, leading to much longer heat exchange times and directly lowering outlet temperature. Moreover, the effect of airflow direction on indoor temperature was not studied. Therefore, it is necessary to further study the influence of the location of the air inlet and outlet of the active heat storage back wall on the temperature of the back wall and the indoor temperature distribution. In particular, it is necessary to find a better air duct layout that can comprehensively improve back wall heat storage, as well as the back wall and indoor temperature distribution.

Due to being convenient to obtain and low-cost, and especially to their good constructability, durability, and thermal insulation capacity, loess walls have been widely adopted in solar greenhouses in Northern China. Therefore, using air ducts arranged in a loess wall for heat exchange and storage to improve thermal performance and thus improve the indoor temperatures of solar greenhouses is of great significance.

Earlier research results of window opening style on the airflow pattern and indoor temperature distribution of solar greenhouses have demonstrated that the high indoor temperature zone during daytime is always located in the upper space of the greenhouse, while the lower temperature zone is in the space close to the ground[14]. Therefore, to transfer the heat of higher temperature indoor air of the greenhouse into the wall through the air duct, the inlet should be preferentially set in the upper space of the greenhouse while the outlet is set close to the ground. On the other hand, considering the limitation of cost and thickness of the wall, the number of air ducts in the wall thickness direction is limited. Moreover, it is conceivable that keeping the cross section area of air duct the same, using distributed small-size air ducts instead of a single larger-size air duct, can effectively improve the limitation of the heat transfer range of a single duct.

In the present work, three kinds of air duct layouts, namely straight-up-and-down duct, fork-shaped top-in-bottom-out distribution duct, and "±"-shaped top-in-side-out distribution duct, were designed. The effect of the layout of the air ducts in loess back wall on the heat transfer and storage characteristics of the back wall was studied using CFD method. Much of the analysis was focused on the reasons for the differences in the characteristics of the heat transfer, the back wall, and indoor temperatures.

2 Materials and simulation method

2.1 Investigated greenhouses

The experimental solar greenhouse with traditional loess walls was located in the Northwest A&F University, Yangling District, Shaanxi, China (34°16′N, 108°06′E). Figure 1 shows the structure of the experimental solar greenhouse. It had a north-south span of 10 m, a length of 10 m, and a height of 5 m. The thickness of the east and west walls was 1.0 m. The back wall had a height of 3.95 m, a thickness of 1.2 m, and its outside was covered with a polystyrene board of 0.10 m in thickness. The front roof was made of thick PO film of 0.10 mm in thickness. The back roof was made of color steel-covered polystyrene board with a total thickness of 100 mm and a width of 1850 mm. The front roof was covered by a thermal insulation quilt made of regenerated cotton with a thickness of 30 mm. The quilt was open from 09:00 to 17:30.

T-type thermocouples (Herouwire and Cable Co. Ltd., Shanghai, China) and Agilent data collector (Agilent Co. Ltd., USA) were adopted to measure the indoor temperature with intervals of 10 min. The indoor temperature measurement points were set at the height of 3.75 m above the ground. HOBO U30 portable automatic meteorological station was adopted to measure the outside air temperature and solar radiation every 1 min. The automatic meteorological station was set up in an open area at the height of 1.5 m above the ground and 0.2 m to the back wall.

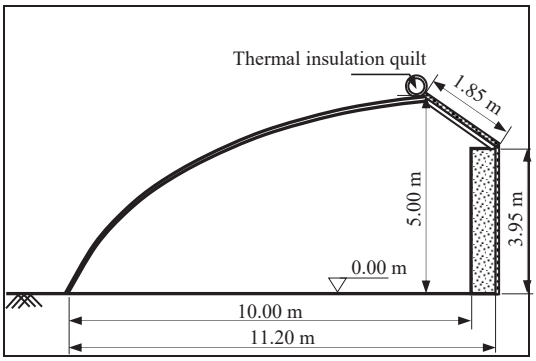

Figure 1 Diagram of solar greenhouse structure

Three kinds of air duct layouts were designed to investigate the effect of the air duct layout in loess back wall on its heat transfer and storage characteristics using CFD method. Figure 2 shows the schematic of the air duct layout. The first one was a straight-up-and-down duct with a length of 3.5 m and denoted by duct (Z) (Figure 2a). The distance from the gable wall to the nearest duct was 2.5 m. The second one was a fork-shaped top-in-bottom-out distribution duct, which was composed of a main vertical duct, a main horizontal duct, and four vertical branch ducts, and denoted by duct (DF) (Figure 2b). The lower end of the main vertical duct was connected in the middle of the horizontal main duct. The lengths of the vertical, horizontal main duct, and vertical branch ducts were 1.3 m, 3.75 m, and 2.2 m, respectively. The distance between distribution branch ducts was 1.25 m, and the distance from the gable wall to the nearest branch duct was 0.625 m. The third one was "±"-shaped with two upper and two lower horizontal branch ducts symmetrically distributed on the two sides of the main duct, and denoted by duct (CF) (Figure 2c). The distances from the upper and lower branch ducts to the inlet were respectively 1.3 m and 2.4 m, and the length of single distribution branch duct was 1.875 m. The distance from the gable wall to the nearest outlet of branch duct was 0.625 m.

The inlets of the three kinds of air duct layouts were all set at 3.7 m above the ground, and the distance between the inlets of ducts was 5 m. The diameter of the main duct was 200 mm, while that of the branch ducts was 100 mm. All of the duct axes were in the plane of the middle of the thickness dimension of the wall.

2.2 CFD modeling of greenhouses

Parametric modeling was conducted using the Geometry module in Ansys Fluent, and 1:1 3D models of the greenhouses were constructed[14,15]. The grid of the overall computing domain of the concerned greenhouse is shown in Figure 3.

The measured values of outdoor solar irradiation and temperature on typical sunny days (November 29-30, 2018) shown in Figure 4 were taken as the external environment parameters for simulation. The Discrete Ordinates (DO) model was chosen to describe the irradiative thermal transfer between inside and outside[16]. During the simulation process, the fan was set to start when the indoor temperature (fan position) was higher than 25ºC in the daytime (09:00-17:30), and stop when indoor temperature was lower than 25ºC.

The air inlet was set as pressure inlet boundary condition, while the air outlets were set as outlet boundary conditions. The air was regarded as an ideal incompressible gas. The inlet air velocity was 0.88 m/s. The flow regime of air in ducts was determined by using

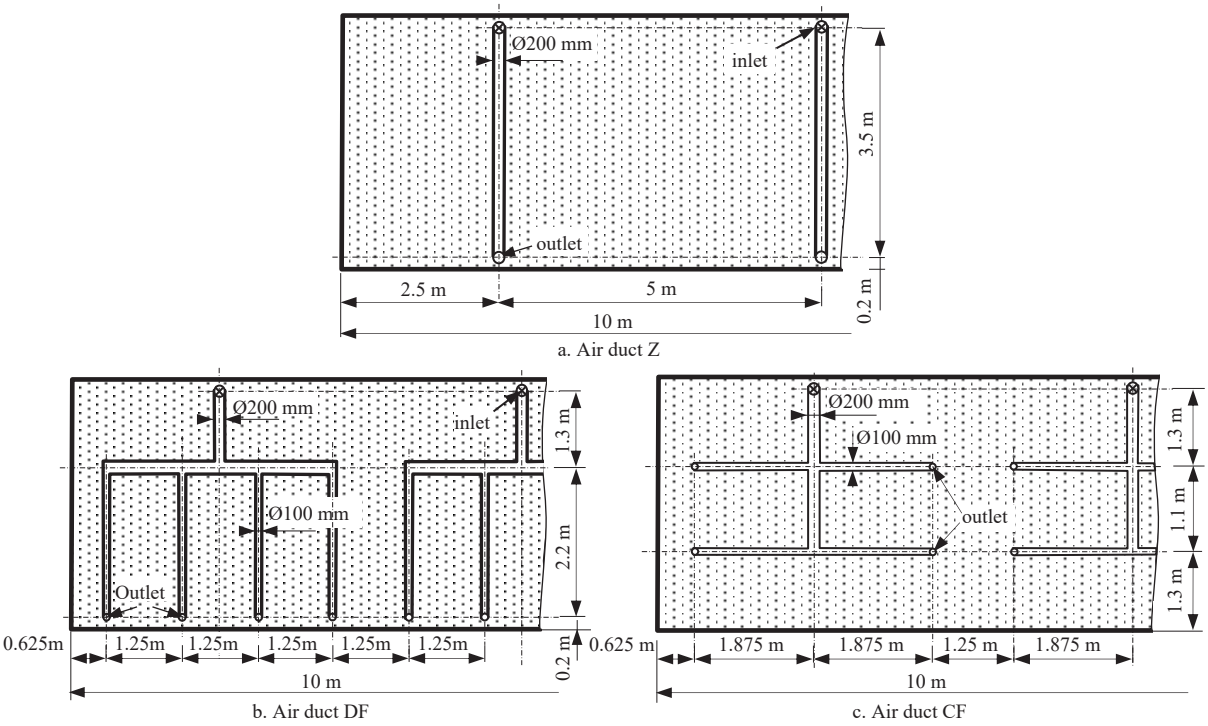

Figure 2 Schematic of layout of air duct in back wall of solar greenhouses

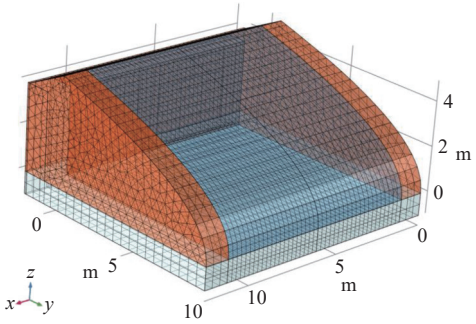

Figure 3 Grid of overall computing domain of concerned greenhouse

Reynolds number, which was calculated by Equation (1)[17]:

$$R_e = \frac{\rho v d}{\mu} \quad (1)$$

where, R_e is the Reynolds number; ρ is the air density, taken as 1.293 kg/m³; v is the air flow velocity, taken as 0.88 m/s; d is the equivalent diameter of the air duct; μ is the air viscosity coefficient, taken as 1.84×10^{-5} m²/s.

According to Equation (1), the Reynolds number in all of the ducts was much higher than 4000 and therefore the air flow should be taken as turbulent flow. The standard k-ε turbulence model was used for the simulating calculation[18]. Table 1 lists the concerned physical properties of the relevant materials used in the simulation.

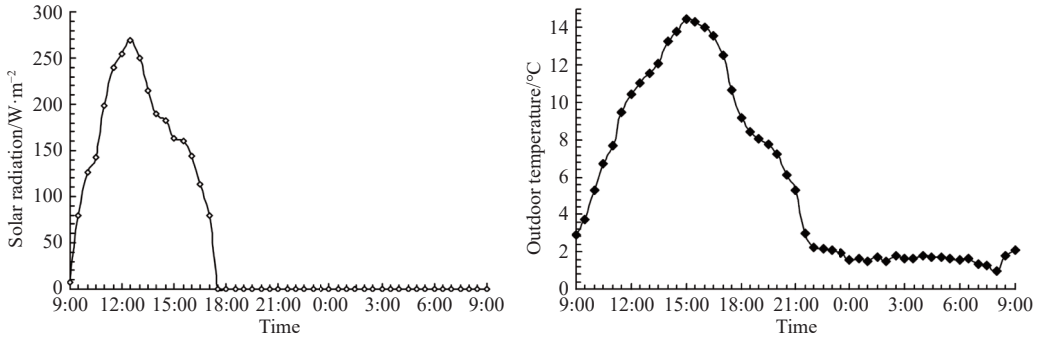

Figure 4 Outdoor solar radiation and outdoor temperature

Table 1 Concerned physical properties of materials used in the simulation

Materials	Density/ (kg·m⁻³)	Thermal conductivity/ (W·m⁻¹·K⁻¹)	Heat capacity/ (J·kg⁻¹·K⁻¹)	Thickness/ m
Air	1.293	0.0242	716.5	-
Soil	1750	1.264	1640	1.2
Loess wall	1050	0.35	1590	1.2
Polystyrene board	350	0.03	1.38	0.1
Thermal insulation quilt	-	0.03	-	0.03
PO plastic film	900	0.29	2550	0.0001

3 Results and discussion

Figure 5 shows the indoor temperature measured in the experimental greenhouse and those simulated in the same greenhouse at the same measurement point. It can be found that the measured and simulated indoor temperatures showed a similar variation tendency. The maximum absolute temperature deviation was 1.97ºC, occurring at 17:30 with a relative deviation of 4.99%. This result indicates that the model can fairly well simulate the indoor temperature of the concerned greenhouse.

Figure 6 shows the air temperature distribution along the ducts

after the fan worked for 5 s. It can be seen that for duct (Z), the air temperature nearly decreased from about 24.83ºC at inlet to about 16.94ºC at outlet. For the two distribution branch ducts, the air temperature distribution along the ducts was both symmetrical with respect to the main inlet duct and decreased as the distance to inlet increased. For duct (DF), the air temperature at the inlet was 24.98ºC, and those at the outlets close to the inner side and the outer side of the main air duct axis were 17.10ºC and 16.94ºC, respectively. For duct (CF), the air temperature at the inlet was 24.84ºC, and those at the upper outlets and the lower outlets were 18.36ºC and 17.22ºC, respectively. Therefore, the temperature difference between the inlet and outlet of duct (Z) was 7.89ºC. The maximum, minimum, and average temperature differences between the inlet and outlets of duct (DF) were 8.04ºC, 7.88ºC, and 7.96ºC, respectively. The maximum, minimum, and average temperature differences between the inlet and outlets of duct (CF) were 7.62ºC, 6.48ºC, and 7.05ºC, respectively. When the hot air passed through the air duct with a lower temperature, heat exchange led to the air temperature decreasing and the heat being stored in the wall. Larger temperature difference between the inlet and outlets of the duct corresponded to higher exchanged heat amounts and heat storage in the wall. Therefore, the above results indicate that the exchanged heat amount of duct (DF) was the highest, while that of duct (CF) was slightly higher than that of duct (Z).

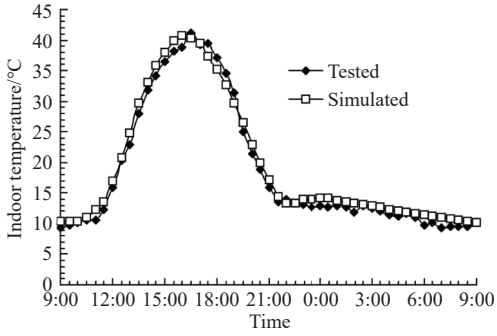

Figure 5 Measured and simulated indoor temperature in experimental greenhouse

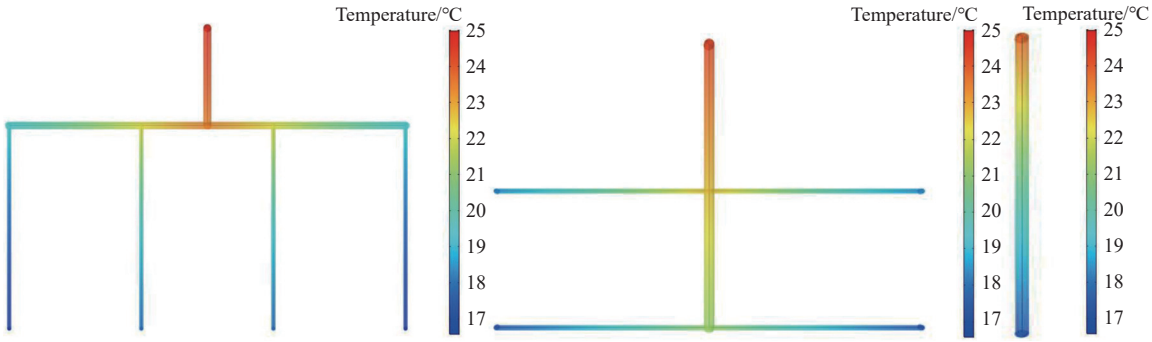

a. The duct DF b. The duct CF c. The duct Z

Figure 6 Temperature distributions along air duct after the fan is started for 5 s

Figure 7 shows the air temperature at outlets and the variations in temperature difference between the inlet and outlets with fan running time. The air temperature at outlets for the three kinds of ducts varied similarly with fan running time, the same as the temperature difference between the inlet and outlets of the ducts. Moreover, at any time, the lowest air temperature at outlets of duct (CF) was the highest. Similarly, and as shown in Figure 6, the air temperature at outlets close to the inner side was higher than that at the outer side of the main air duct axis for duct (DF), while the air temperature at the upper outlets was higher than that at the lower outlets for duct (CF). In addition, the maximum temperature difference between the inlet and outlet of duct (Z) was 13.64ºC. The maximum temperature difference between the inner and outer side outlets was 1.23ºC, and the maximum temperature differences between the inlet and the inner distribution branch duct outlets and outer distribution branch outlets of duct (DF) were 14.87ºC and 13.64ºC, respectively. The maximum temperature difference between the upper and lower outlets was 1.65ºC, and the maximum temperature differences between the inlet and upper and lower distribution branch duct outlets of duct (CF) were 13.06ºC and 11.42ºC, respectively. The above results also indicate that during the heat storage process, the exchanged heat amount of duct (DF) was the highest, while that of duct (Z) was the lowest.

Figure 8 shows the temperature distribution of the wall on the air duct plane at the time the fan was stopped. It can be seen that the wall temperature of the upper zone with a width of about 0.5 m was higher, but that of the lower zone near the foot of the wall was lower. For the traditional passive heat storage wall, the temperature was layered distribution; it notably decreased from 24ºC to 19.0ºC in the upper zone, then it gradually decreased to about 14.5ºC at the foot of the wall. The temperature of the back wall was mainly in the range of about 15.5ºC-16.5ºC. For the back wall with duct (Z), the temperature distribution was T-shaped. The temperature in the upper zone was in the range of about 19.5ºC-24.8ºC. The temperature around the duct was about 18.3°C-19.0°C, and it decreased with the decrease of the distance to the wall of duct and wall height. The temperature in the other zone was in the range of about 15.5ºC-17.5ºC. On the whole, the temperature of the back wall with duct (Z) was mainly in the range of about 16ºC-17.5ºC. For the back wall with duct (DF), the temperature in the upper zone was in the range of about 22.5ºC-23.5ºC, while that in the zone downward of the horizontal duct was in the range of 18.5ºC-21.5ºC, mainly between about 18.5ºC-20.5ºC. The temperature between the distribution branch ducts was relatively uniform and ranged from about 17.1ºC-17.6ºC. The temperature at the foot of the wall was 14.8ºC. On the whole, the temperature of the back wall with duct (DF) was mainly in the range of about 17ºC-19ºC. For the back wall with duct (CF), the temperature in the upper zone was in the range of 19ºC-23.5ºC, and that in the zone downward of the upper horizontal distribution branch ducts was in the range of about 18ºC-19ºC. The temperature between the upper and lower distribution branch ducts was mainly in the range of about 17ºC-18ºC. The temperature in the other zone was in the range of about 14.5ºC-16C. On the whole, the temperature of the back wall with duct (CF) was

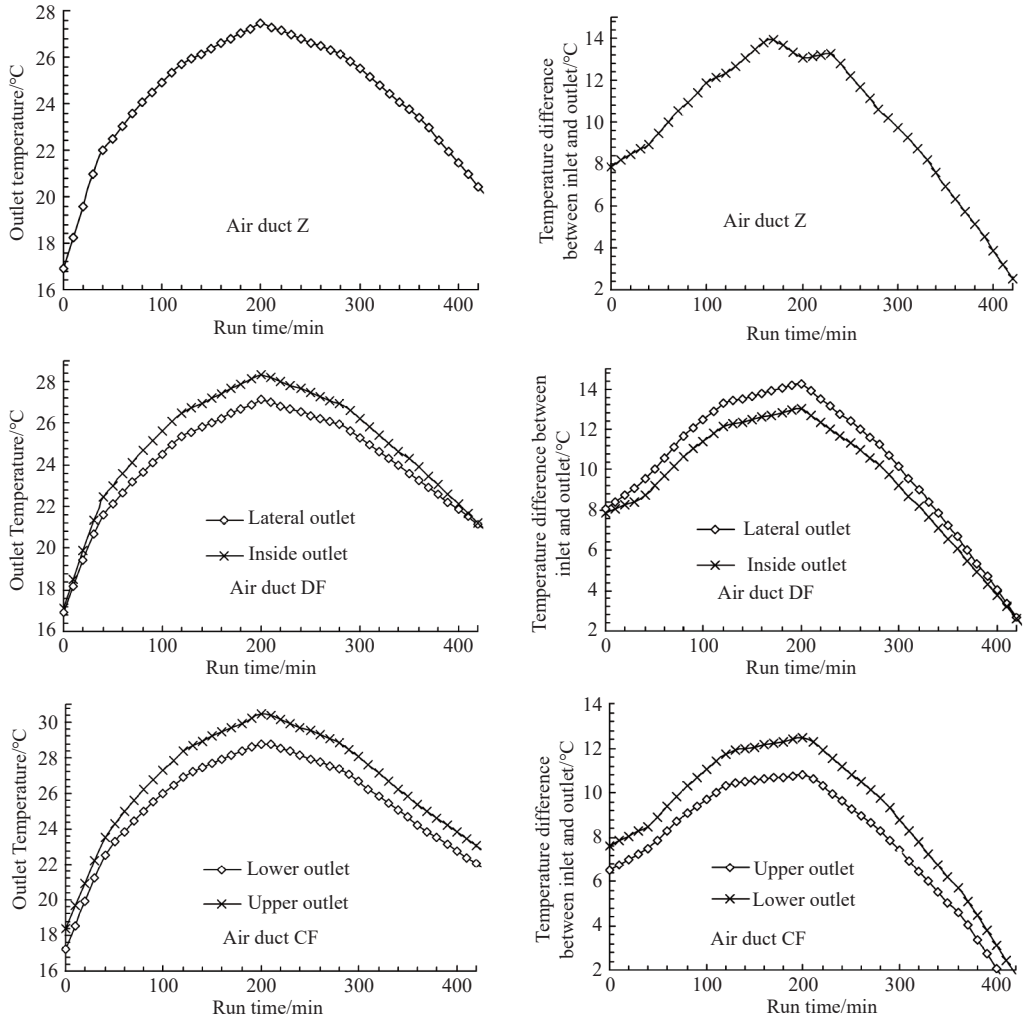

Figure 7 Outlet temperature and temperature difference between inlet and outlets of the three kinds of air ducts and their variations with fan running time

mainly in the range of about 16ºC-18ºC.

The different types of backwalls and ducts significantly affected the thermal performance of solar greenhouse[19,20]. In general, the temperature of the active heat storage wall was higher than that of the passive heat storage wall. Moreover, the back wall with duct (DF) showed the highest overall temperature and the best uniform temperature distribution. The overall temperature and distribution uniformity of the back wall with duct (CF) were higher and better than those of the back wall with duct (Z). The distribution duct is favorable for improving the amount and range of heat storage in the wall.

The exchanged heat amount between the hot air and the back wall through the air duct can be described as[21,22]:

$$Q = \int_l q_x A t \mathrm{d}x = -\int_l \lambda \frac{\partial T}{\partial x} A t \mathrm{d}x = \lambda A t \int_l \Delta T(x) \mathrm{d}x \tag{2}$$

where, λ was the thermal conductivity of air duct, A was heat exchange area of air duct, $\frac{\partial T}{\partial x}$ was the temperature difference between two sides of air duct wall at the section located at a distance of x from the air duct inlet, and t was the duration of heat exchange.

In the present work, the materials of back wall and air duct were the same. The thermal conductivity of the three kinds of air ducts was the same. The heights of the inlet and outlet of duct (DF) and duct (Z) were respectively the same. The initial temperature at the inlet and outlet for every air duct layout was nearly the same. Moreover, the initial temperature at the top of the distribution ducts close to the main duct was nearly the same as that at the bottom of main duct of duct (DF). Consequently, it can be considered that the temperature difference between the two sides of the air duct wall along the whole duct, $\Delta T(x)$ for duct (DF) and duct (Z) was the same.

The heat exchange area of ducts (Z) and (DF), A_Z and A_{DF} can be described as

$$A_Z = \pi D l \tag{3}$$

$$A_{DF} = \pi D l_m + 4\pi d l_d \tag{4}$$

where, l is the length of duct (Z). D and d are the diameter of the main duct and branch ducts of duct (DF), respectively. l_m and l_d are the length of the main duct and branch ducts of duct (DF), respectively.

From Figure 2, it can be obtained that the lengths and diameters of the concerned air ducts were l=3.5 m, D=200 mm, d=100 mm; l_m=1.3 m; l_d=2.2 m, respectively. It can be calculated that the ratio of duct (DF), A_{DF} to that of duct (Z), A_Z was A_{DF} : A_Z=5.7: 3.5. On the other hand, it can be obtained that the time for the air flow through duct (Z), τ_Z was about 3.98 s, while the average time for the air flow through duct (DF), τ_{DF} was about 5.40 s. Therefore, it can be conceivable that during the same period, the heat exchange frequency of the former was higher. Consequently, in the same period of time Δt, the ratio of exchanged heat amount in the back wall with duct (DF) to that in the back wall with duct (Z) can be

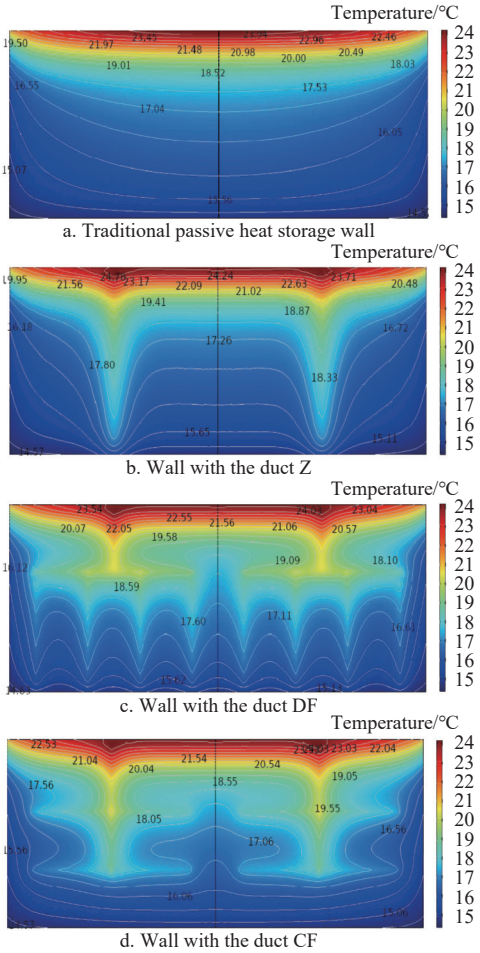

a. Traditional passive heat storage wall

b. Wall with the duct Z

c. Wall with the duct DF

d. Wall with the duct CF

Figure 8 Temperature distribution of wall on air duct plane at the time of fan being stopped

expressed as

$$\frac{Q_{DF}}{Q_Z}=\frac{A_{DF}\Delta t/\tau_{DF}}{A_Z\Delta t/\tau_Z}=\frac{5.7}{3.5}\times\frac{3.98}{5.40}\partial 1.2 \quad (5)$$

Therefore, during the same period, the exchanged heat amount in the back wall with duct (DF) was clearly greater than that of the back wall with duct (Z).

It can be obtained that the ratio of the heat exchange area of duct (CF) A_{CF} to that of duct (Z) was A_{CF} : A_Z=6.15: 3.5. However, it should be noted that the average air temperature difference between the inlet and outlet of duct (CF), ΔT_{CF} was lower than that of duct (Z), ΔT_Z and the ratio was about ΔT_{CF}: ΔT_Z=1: 1.35. On the other hand, the average time for the air flow through duct (CF), τ_{CF} was about 4.85 s, which was clearly longer than that for the air flow through duct (Z). Assuming the temperature difference between two sides of the air duct wall varied linearly along the duct, then according to Equation (4), the ratio of exchanged heat amount in the back wall with duct (CF) to that in the back wall with duct (Z) can be expressed as

$$\frac{Q_{CF}}{Q_Z}=\frac{A_{CF}\Delta t/\tau_{CF}}{A_Z\Delta t/\tau_Z}\times\frac{\Delta T_{CF}}{\Delta T_Z}=\frac{6.15}{3.5}\times\frac{3.98}{4.85}\times\frac{1}{1.35}\partial 1.07 \quad (6)$$

As a result, in the same period of time, the exchanged heat amount in the back wall with duct (DF) was the highest, while that in the back wall with duct (CF) was slightly higher than that in the back wall with duct (Z).

Figure 9 shows the lowest, highest, and average indoor temperature of the greenhouse with different air duct layouts in the back wall on a typical sunny day and night (based on Nov. 29-30, 2018). It can be seen that the highest indoor temperature of the four kinds of greenhouses was very close, but the highest average indoor temperature of the greenhouse with the traditional passive heat storage wall was much higher than those of the greenhouses with active heat storage walls. The highest and the lowest average indoor temperature of the greenhouse with the traditional passive heat storage wall were respectively about 46.52ºC and 31.33ºC. The highest and the lowest average indoor temperatures of the greenhouses with the active heat storage walls with the duct (DF), the duct (CF), and the duct (Z) were about 44.86ºC and 31.12ºC, 46.29ºC and 31.25ºC, and 46.36ºC and 31.18ºC, respectively.

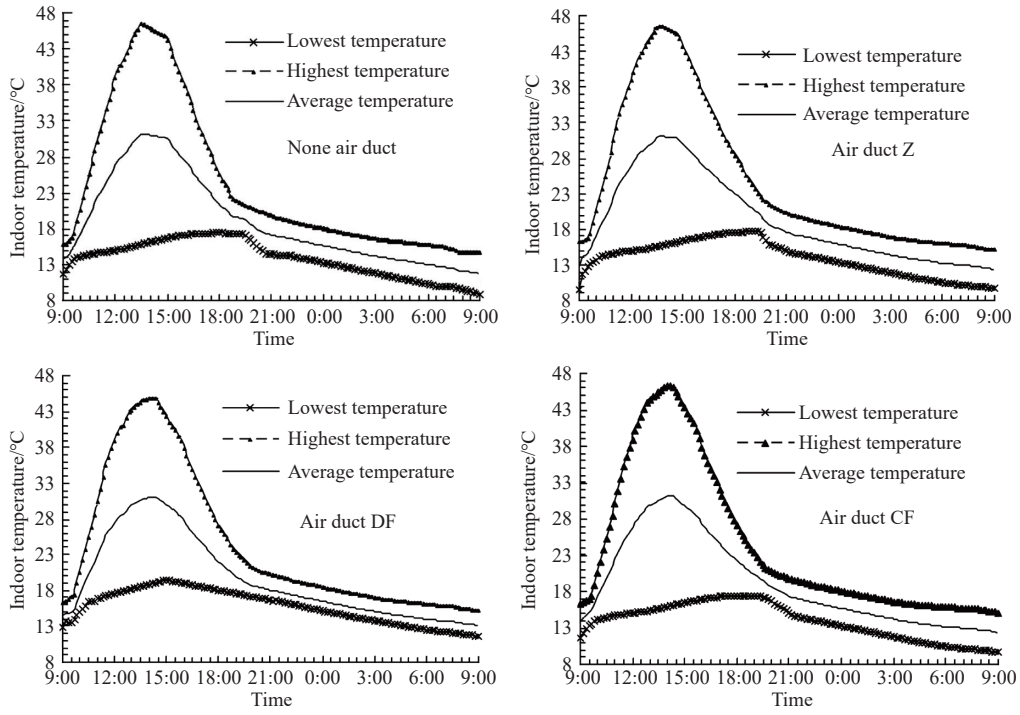

Figure 9 Lowest, highest, and average indoor temperatures of the greenhouse with different air ducts in back wall on a typical sunny day and night (based on 2018.11.29-30)

After the fan started in the daytime, the hot air was continuously poured into the air duct located in the back wall with lower temperature and exchanged heat with the back wall. Therefore, the temperature of the air flowing out of the air duct was reduced and the heat stored in the back wall. Meanwhile, the recurrence of hot air inflow and lower temperature air outflow gradually slowed down the rise of indoor temperature. However, the temperature of the air flowing out of the air duct was still higher than that of the temperature in the lower space of the greenhouse. Therefore, the lowest and average indoor temperature gradually increased with time (solar irradiation increasing). Additionally, the higher the exchanged heat amount, the bigger the temperature drop of inlet and outlet air, and the more obvious the increase of lowest or average indoor temperature. The greenhouse with the active heat storage wall with the duct (DF) showed the biggest temperature drop between the inlet and outlet air and average indoor temperature increment, suggesting the duct (DF) had the best heat transfer and storage effect. Similarly, the heat transfer and storage effect of the back wall with the duct (CF) was slightly better than that of the back wall with the duct (Z), as the former showed slightly higher average indoor temperature but lower highest indoor temperature.

During the exothermic process at night, the indoor temperature gradually and quasi-linearly decreased with increasing time and showed the lowest value at about the next 9:00 a.m. The lowest, highest, and average indoor temperatures of the greenhouse with the traditional passive heat storage wall at the next 9:00 a.m. were about 8.92ºC, 14.61ºC, and 11.65ºC, respectively. The lowest, highest, and average indoor temperatures of the greenhouse with the active heat storage wall with the duct (DF) at the next 9:00 a.m. were about 11.48ºC, 15.06ºC, and 13.41ºC, respectively. The lowest, highest, and average indoor temperatures of the greenhouse with the active heat storage wall with the duct (CF) at the next 9:00 a.m. were about 9.63ºC, 14.98ºC, and 12.31ºC, respectively. The lowest, highest, and average indoor temperatures of the greenhouse with the active heat storage wall with the duct (Z) at the next 9:00 a.m. were about 9.62ºC, 14.96ºC, and 12.28ºC, respectively. Therefore, compared to the greenhouse with the traditional passive heat storage wall, the greenhouse with the active heat storage wall showed improved indoor temperatures during the day and night. The optimal duct layout was the top-in-bottom-out distribution duct (DF), which had the most obvious increase in lowest indoor average temperature of about 1.76ºC, as well as more uniform temperature. Table 2 lists typical indoor temperatures corresponding to the moment of the highest temperature during the heat storage process and to the moment of the lowest temperature during the exothermic process.

Table 2 Typical indoor temperatures corresponding to the highest temperature moment during the heat storage process and to the lowest temperature moment during the exothermic process (ºC)

Air duct layout	Heat storage process			Exothermic process			
	Lowest	Highest	Average	Lowest	Highest	Average	Difference
None	16.13	46.52	31.33	8.92	14.61	11.65	5.69
DF	19.02	44.86	31.12	11.48	15.06	13.41	3.58
CF	16.00	46.36	31.18	9.63	14.98	12.31	5.37
Z	16.21	46.29	31.25	9.62	14.96	12.28	5.33

CFD has been widely used in greenhouse thermal environment simulation and ventilation simulation[23-26]. Researchers have also applied it to simulate the thermal and humidity environment of Chinese solar greenhouses and the impact of different building parameter values on the environment[27-29]. Figure 10 shows the temperature distribution of the middle cross section of the greenhouse with different duct types at the next 9:00 a.m. using CFD simulation. It seems that the temperature distribution in the greenhouse was stratified, and the temperature near the front roof was the lowest, which was the low-temperature area (blue area in Figure 10). Moreover, the low-temperature area of the greenhouse with an active heat storage wall was basically equivalent, which was smaller than that of the greenhouse with the traditional passive heat storage wall. The temperature near the wall was the highest, especially in the triangle area below 1/2 of the wall height and 2/5 forward of the ground, which was the high-temperature area (yellow area in Figure 9). The average temperatures at the low-temperature area and the high-temperature area of the greenhouse with a traditional passive heat storage wall were 10.58ºC and 13.96ºC, respectively. The average temperatures at the low-temperature area and the high-temperature area of the greenhouse with an active heat storage wall with duct (DF) were 11.02ºC and 14.46ºC, respectively. The average temperatures at the low-temperature area and the high-temperature area of the greenhouse with an active heat storage wall with duct (CF) were 10.86ºC and 14.35ºC, respectively. The average temperatures at the low-temperature area and the high-temperature area of the greenhouse with an active heat storage wall with duct (Z) were 10.82ºC and 14.05ºC, respectively.

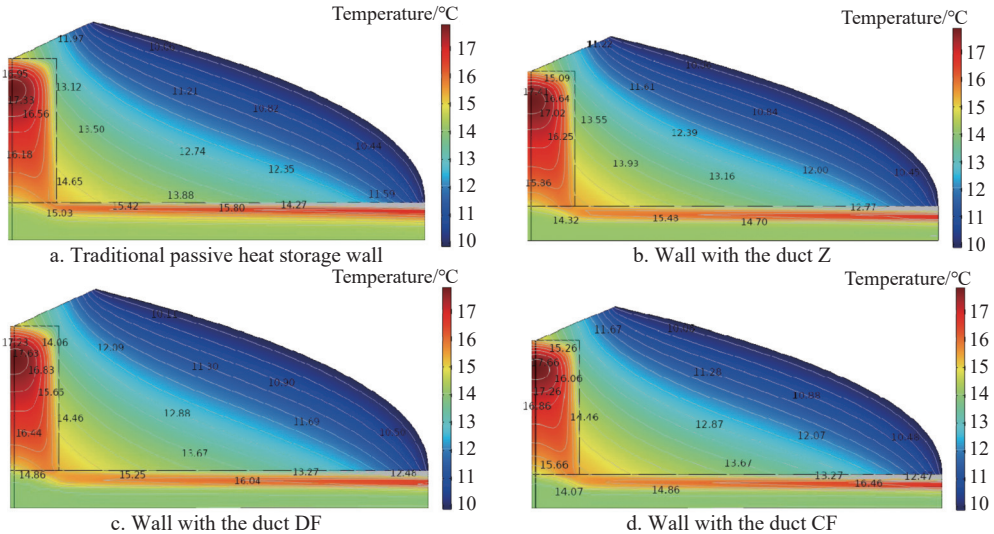

a. Traditional passive heat storage wall b. Wall with the duct Z

c. Wall with the duct DF d. Wall with the duct CF

Figure 10 Temperature distribution of middle cross section of greenhouse at the next 9:00 a.m. (Nov. 30, 2018)

On the other hand, from Figure 10, it can be found that the indoor temperature at the position close to the front roof with the same distance from different greenhouses also showed similar characteristics. For example, the indoor temperatures at the 3rd isotherm corresponding to the solar greenhouse without air duct, and with air duct Z, DF, and CF were 10.82ºC, 10.84ºC, 10.90ºC, and 10.88ºC, respectively. The indoor temperatures at the 4th isotherm corresponding to the solar greenhouse without air duct, and with air duct Z, DF, and CF were 11.21ºC, 11.22ºC, 11.30ºC, and 11.28ºC, respectively.

The above results also indicate that the active heat storage wall is favorable to the enhancement of the indoor temperature and its uniformity. Duct (DF) had the best heat transfer and storage effect. The heat transfer and storage effect of the back wall with duct (CF) was slightly better than that of the back wall with duct (Z).

4 Conclusions

In the same period of time, the transferred heat amount in the back wall with the top-in-bottom-out distribution duct (DF) was the largest, while that in the back wall with the top-in-side-out distribution duct (CF) was slightly higher than that of the back wall with the top-in-bottom-out with straight-up-and-down duct (Z).

The temperature of the active heat storage wall was higher than that of the passive heat storage wall. The distribution duct is favorable for improving the heat storage range of the wall. The back wall with the top-in-bottom-out distribution duct (DF) showed the lowest overall temperature at daytime, the highest at night, and the most uniform temperature distribution.

The optimal duct among the three kinds of active heat storage duct layouts is the top-in-bottom-out distribution duct (DF). The greenhouse with the duct (DF) in the back wall showed the most obvious increase in the indoor average temperature, the highest temperature at night, and the most uniform temperature.

Acknowledgements

This research was financially supported by the National Natural Science Foundation of China (31901420), Jiangsu Provincial Natural Science Foundation (Grant No. BK20241174), and Key Research and Development Program Project of Ningxia Hui Autonomous Region (2023BCF01022).

[References]

[1] Wu G, Zhang Y, Fang H, Yang Q C. Study on application status of solar thermal technology in solar greenhouse of China. Acta Horticulturae, 2020; 1296: 9–16.

[2] Li M, Wang P Z, Song W T. Feasibility of employing a heat insulation wall as the north wall of a Chinese solar greenhouse in a severely cold area of China. Applied Engineering in Agriculture, 2019; 35(6): 903–910.

[3] Liu X G, Li Y M, Liu A H, Yue X, Li T L. Effect of north wall materials on the thermal environment in Chinese solar greenhouse (Part A: experimental researches). Open Physics, 2019; 17(1): 752–767.

[4] Ren J, Zhao Z, Zhang J, Wang J, Guo S R, Sun J. Study on the hygrothermal properties of a Chinese solar greenhouse with a straw block north wall. Energy and Buildings, 2019; 193: 127–138.

[5] Zhang G P, Shi Y L, Liu H, Fei Z Y, Liu X, Wei M, et al. Heat transfer performance of an assembled multilayer wall in a Chinese solar greenhouse considering humidity. Journal of Energy Storage, 2021; 33(1): 102046.

[6] Liu X G, Li H, Li Y M, Yue X, Tian S B, Li T L. Effect of internal surface structure of the north wall on Chinese solar greenhouse thermal microclimate based on computational fluid dynamics. PLoS One, PLoS One, 2020; 15(4): e0231316.

[7] Bezari S, Bekkouche S, Benchatti A. Investigation and improvement for a solar greenhouse using sensible heat storage material. FME Transactions, 2021; 49(1): 154–162.

[8] Han F T, Chen C, Hu Q L, He Y P, Wei S, Li C Y. Modeling method of an active–passive ventilation wall with latent heat storage for evaluating its thermal properties in the solar greenhouse. Energy and Buildings, 2021; 238: 110840.

[9] Zhao S M, Zhuang Y F, Zheng K X, Ma C W, Cheng J Y, Ma C, Chen X W, Zhang T Z. Thermal performance experiment on air convection heat storage wall with cavity in Chinese solar greenhouse. Transactions of the CSAE, 2018; 34(4): 223–231. (in Chinese)

[10] Bo Z, Yi Z, Yang Q, Hui F, Wei L, Sheng Z. Dehumidification in a chinese solar greenhouse using dry outdoor air heated by an active heat storage-release system. Applied Engineering in Agriculture, 2016; 32(4): 447–456.

[11] Kuroyanagi T. Current usage of air circulators in greenhouses in Japan. Jarq-japan Agricultural Research Quarterly, 2016; 50(1): 7–12.

[12] Zhang Y, Gao W B, Zou Z R. Performance experiment and CFD simulation of heat exchange in solar greenhouse with active thermal storage back wall. Transactions of the CSAE, 2015; 31(5): 203–211. (in Chinese)

[13] Bao E C, Zou Z Y, Zhang Y. CFD simulation of heat transfer in back-wall of active thermal-storage solar greenhouse with different airflow directions. Transactions of the CSAE, 2018; 34(22): 169–177. (in Chinese)

[14] Sun Y C, Bao E C, Zhu C M, Yan L L, Cao Y F, Zhang X H, Li J M, Jing H W, Zou Z R. Effects of window opening style on inside environment of solar greenhouse based on CFD simulation. Int J Agric & Biol Eng, 2020; 13(6): 53–59.

[15] He F, Si C Q, Ding X M, Gao Z J, Gong B B, Qi F, et al. Optimization of Chinese solar greenhouse building parameters based on CFD simulation and entropy weight method. Int J Agric & Biol Eng, 2023; 16(6): 48–55.

[16] Nguyen Q, Hashemi B M, Amir P, Omid M, Arash K. Discrete ordinates thermal radiation with mixed convection to involve nanoparticles absorption, scattering and dispersion along radiation beams through the nanofluid. Journal of Thermal Analysis and Calorimetry, 2021; 143(3): 2801–2824.

[17] Lu H, Zhang L Z. Particle deposition characteristics and efficiency in duct air flow over a backward-facing step: analysis of influencing factors. Sustainability, 2019; 11(3): 751–768.

[18] Omer A Alawi, Abdelrazek A H, Aldlemy M S, Ahmed W, Hussein O A, Ghafel S T, et al. Heat transfer and hydrodynamic properties using different metal-oxide nanostructures in horizontal concentric annular tube: an optimization study. Nanomaterials, 2021; 11(8): 1979.

[19] Sun Y C, Wang H T, Zhu C M, Lyu H Y, Zhang X H, Cao Y F, et al. Application performances of two greenhouses with new types of backwall in Yangling, China. Int J Agric & Biol Eng, 2022; 15(3): 62–71.

[20] Cao Y F, Xu H J, Shi M, Zhang X Y, Zhang Y H, Zou Z R. Analysis of the thermal performance of the novel assembled Chinese solar greenhouse with a modular soil wall in winter of Yinchuan, China. Int J Agric & Biol Eng, 2022; 15(5): 70–77.

[21] Sobota T. Fourier's law of heat conduction. Springer Netherlands, 2014.

[22] Du B X, Xu G Y, Xue D W, Wang J B. Fractional thermal wave bio-heat equation based analysis for living biological tissue with non-Fourier Neumann boundary condition in laser pulse heating. Optik, 2021; 247: 167811.

[23] Li H, Ji D, Hu X, Xie T, Song W T, Tian S B. Comprehensive evaluation of combining CFD simulation and entropy weight to predict natural ventilation strategy in a sliding cover solar greenhouse. Int J Agric & Biol Eng, 2021; 14(6): 213–221.

[24] Gao Z J, Li W Y, Li W, Ding X M. Experimental research on the microclimate in the naturally ventilated multi-span greenhouse. Int J Agric & Biol Eng, 2024; 17(3): 68–74.

[25] Zhang G X, Fu Z T, Yang M S, Liu X X, Dong Y H, Li X X. Nonlinear simulation for coupling modeling of air humidity and vent opening in Chinese solar greenhouse based on CFD. Computers and Electronics in Agriculture, 2019; 162: 337–347.

[26] He X L, Wang J, Guo S R, Zhang J, Wei B, Sun J, et al. Ventilation optimization of solar greenhouse with removable back walls based on CFD. Computers and Electronics in Agriculture, 2018; 149: 16–25.

[27] Zhang X, Wang H L, Zou Z R, Wang S J. CFD and weighted entropy based simulation and optimisation of Chinese solar greenhouse temperature distribution. Biosystem Engineering, 2016; 142: 12–26.

[28] Tong G H, Christopher D M, Li B M. Numerical modelling of temperature variations in a Chinese solar greenhouse. Computers and Electronics in Agriculture, 2009; 68: 129–139.

[29] Li Y M, Liu X G, Qi F S, Wang L, Li T L. Numerical investigation of the north wall passive thermal performance for Chinese solar greenhouse. Thermal Science, 2020; 24(6A): 3465–3476.